Electronic Supplementary Material (ESI) for Nanoscale.

Supporting Information

N-gene-Complementary Antisense-Oligonucleotides Directed Molecular Aggregation of Dual-Colour Carbon Dots, Leading to Efficient Fluorometric Sensing of SARS-COV-2 RNA

Zach Sheffield,[a] Maha Alafeef,[a,b,c,d] Parikshit Moitra,[a,b] Priyanka Ray,[a,b] Dipanjan Pan*[,a,b,c,e]

[a] Department of Chemical, Biochemical and Environmental Engineering, University of Maryland Baltimore County, 1000 Hiltop Circle, Baltimore, Maryland 21250, USA

[b] Center for Blood Oxygen Transport and Hemostasis, Department of Pediatrics, University of Maryland Baltimore School of Medicine, 670 W Baltimore St., Baltimore, Maryland 21201, USA

[c] Bioengineering Department, University of Illinois at Urbana-Champaign, Illinois 61801, USA

[d] Biomedical Engineering Department, Jordan University of Science and Technology, Irbid 22110, Jordan

[e] Department of Diagnostic Radiology and Nuclear Medicine, University of Maryland Baltimore, 670 West Baltimore Street, Baltimore, Maryland 21201, United States

*Correspondence: dipanjan@som.umaryland.edu

Table of contents **Page No.**

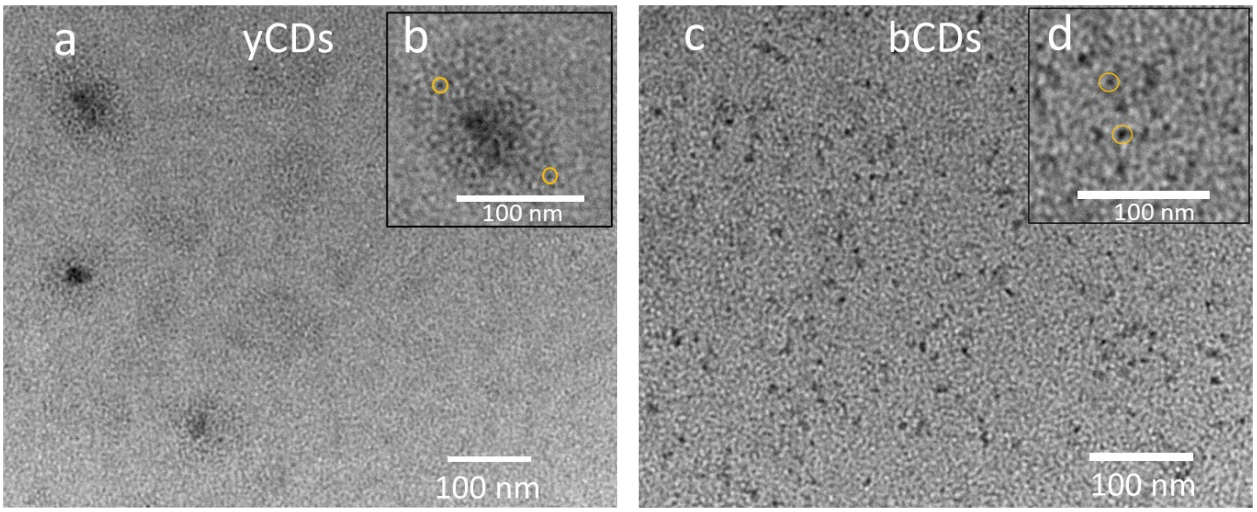

Figures.

Supplementary Figure S1. Representative TEM images of yCDs (a-b) and bCDs (c-d) before ASO-conjugation. Yellow circles in the insets b and d were included to denote the representative particles.

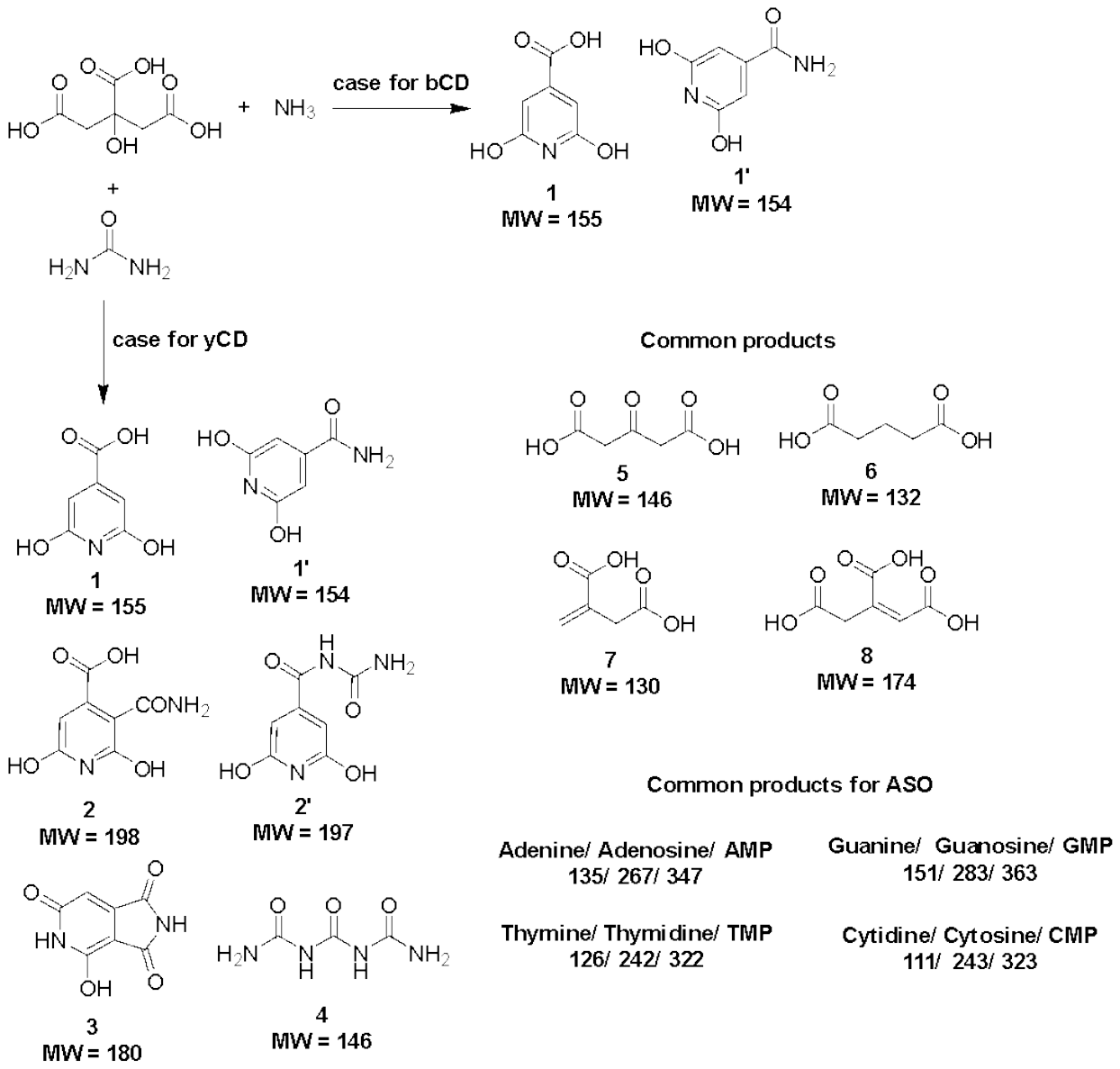

Supplementary Figure S2. Common, expected products from the synthesis of yCDs (reaction between citric acid and urea), the synthesis of bCDs (reaction between citric acid and ammonia), and the fragmentation of the antisense oligonucleotides. AMP, GMP, TMP, and CMP respectively stand for adenine monophosphate, guanine monophosphate, threonine monophosphate, and cytosine monophosphate.

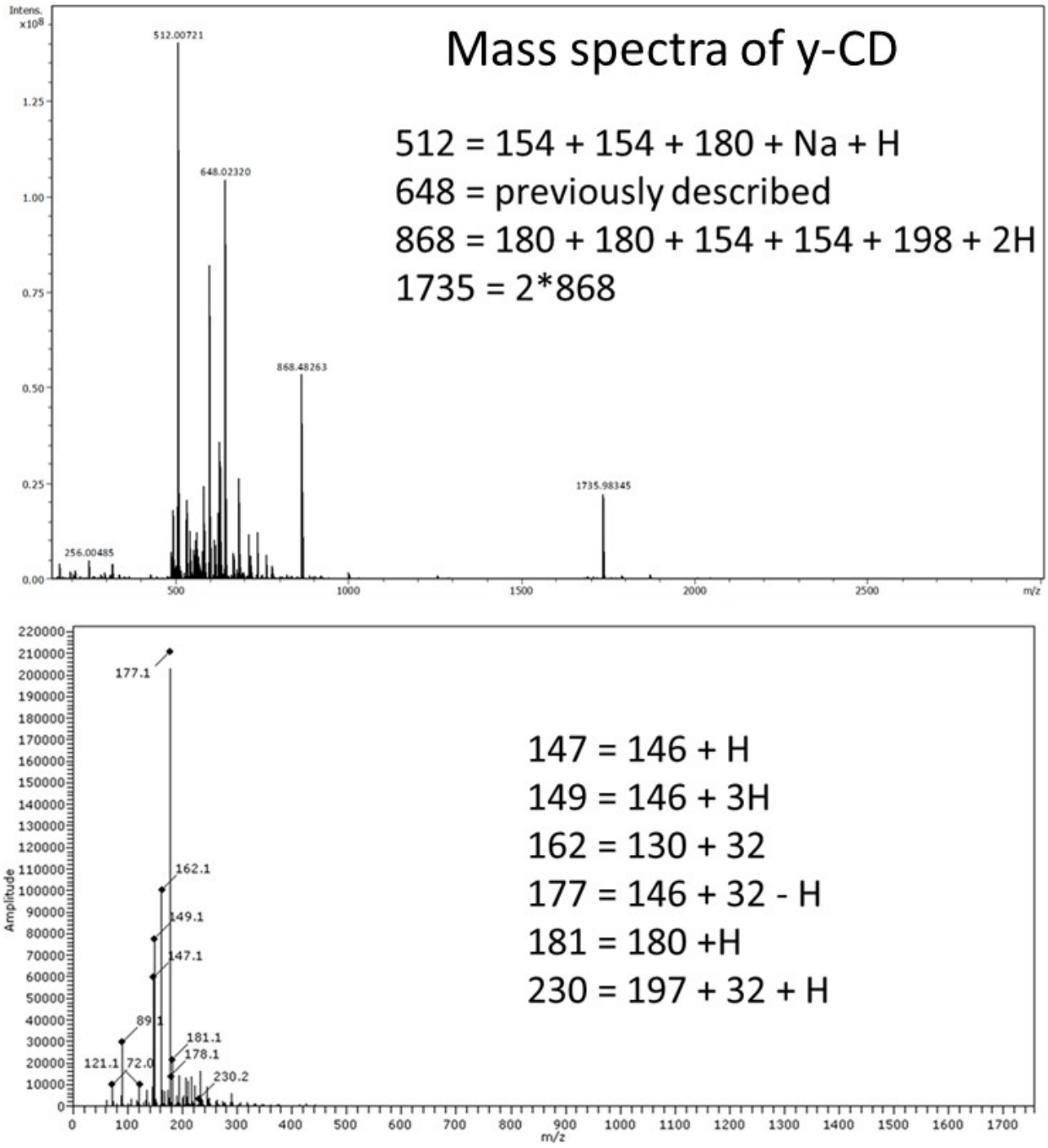

Supplementary Figure S3. High-resolution MALDI and ESI TOF mass spectroscopy data of yCDs.

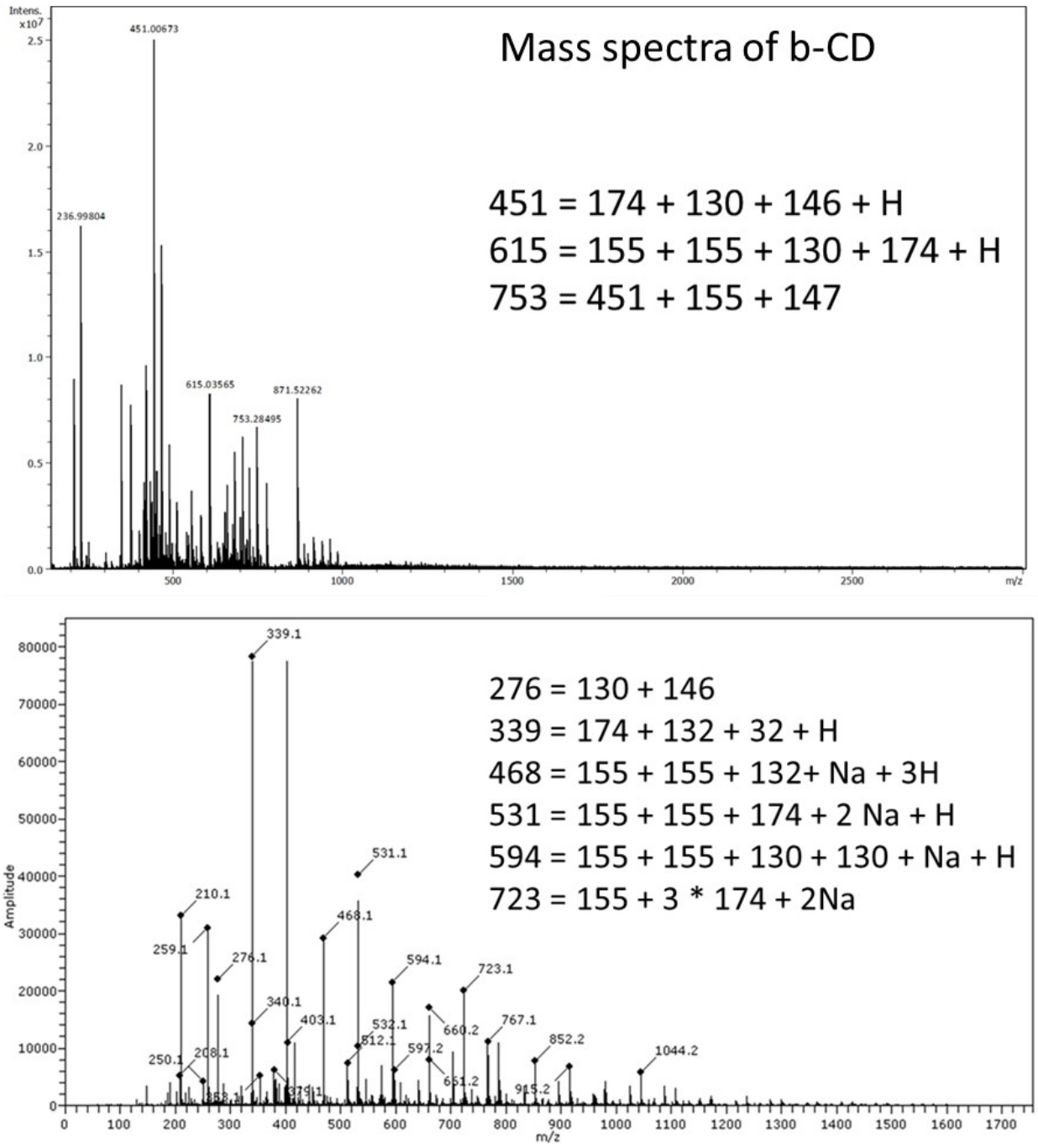

Supplementary Figure S4. High-resolution MALDI and ESI-TOF mass spectroscopy data of bCDs.

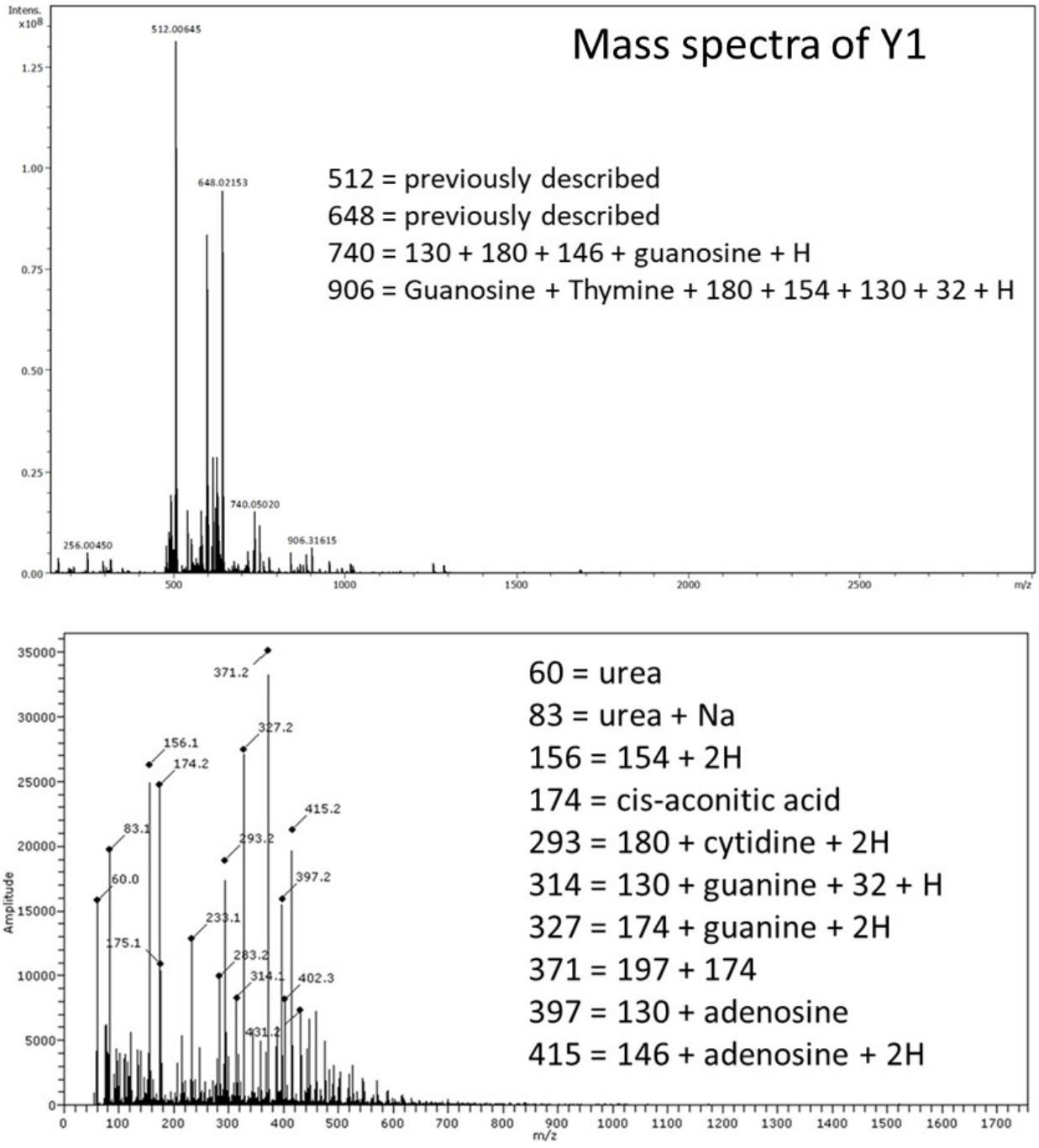

Supplementary Figure S5. High-resolution MALDI and ESI-TOF mass spectroscopy data of Y1s.

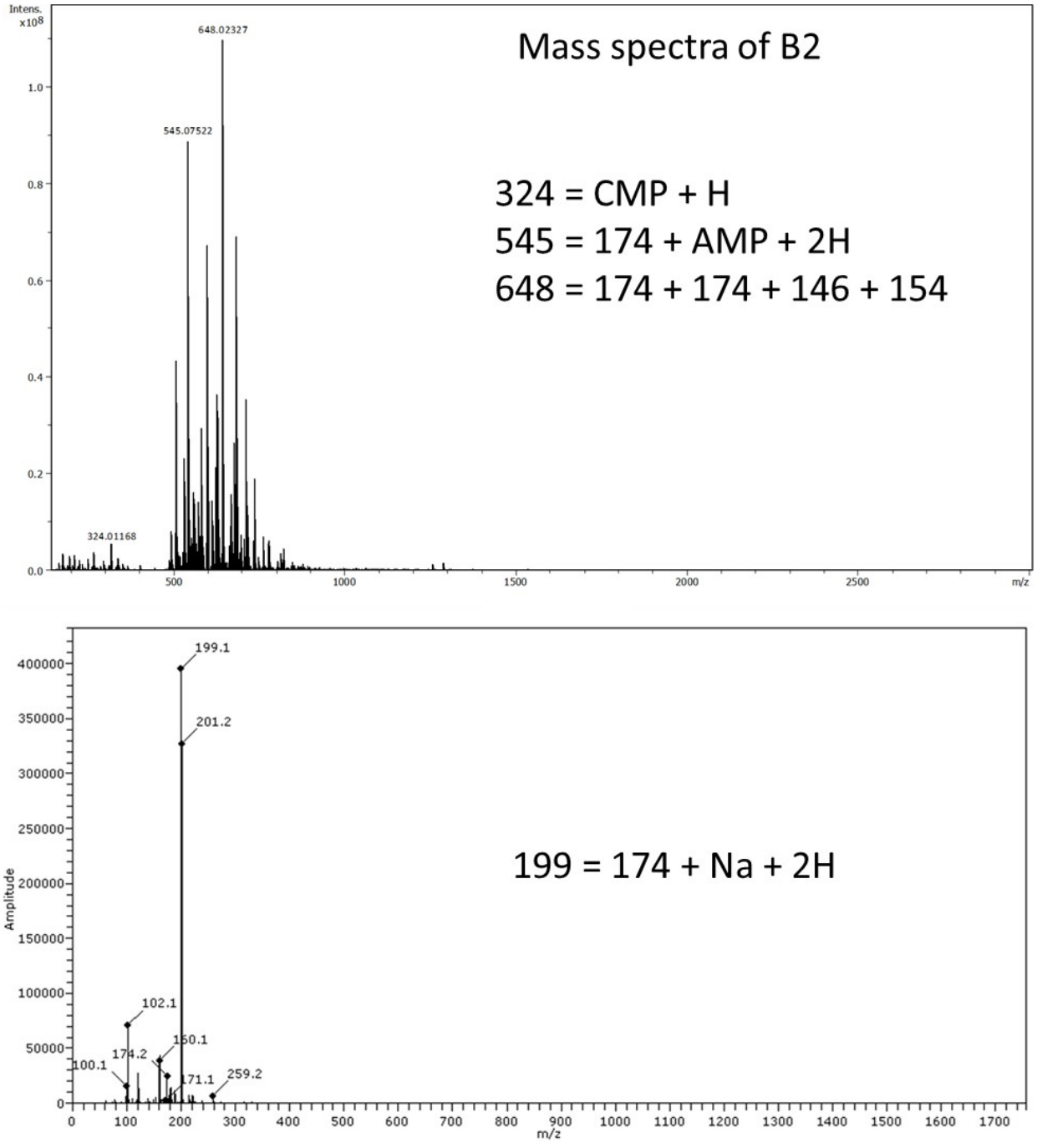

Supplementary Figure S6. High-resolution MALDI and ESI-TOF mass spectroscopy data of B2.

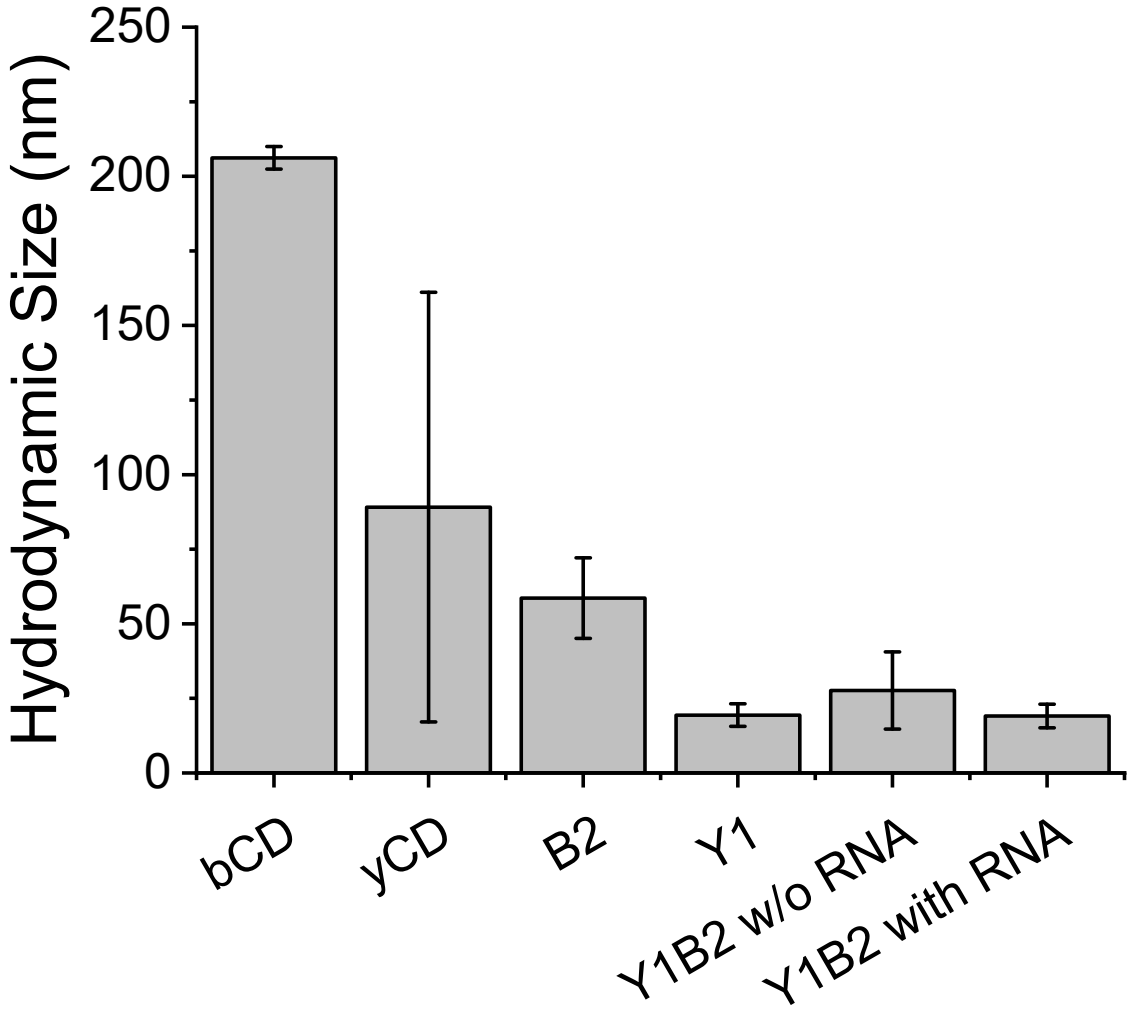

Supplementary Figure S7. The DLS measured number-averaged hydrodynamic sizes of bCDs, yCDs, B2s, Y1s, the Y1B2 mixture without SARS-CoV-2 RNA, and Y1B2 with RNA.

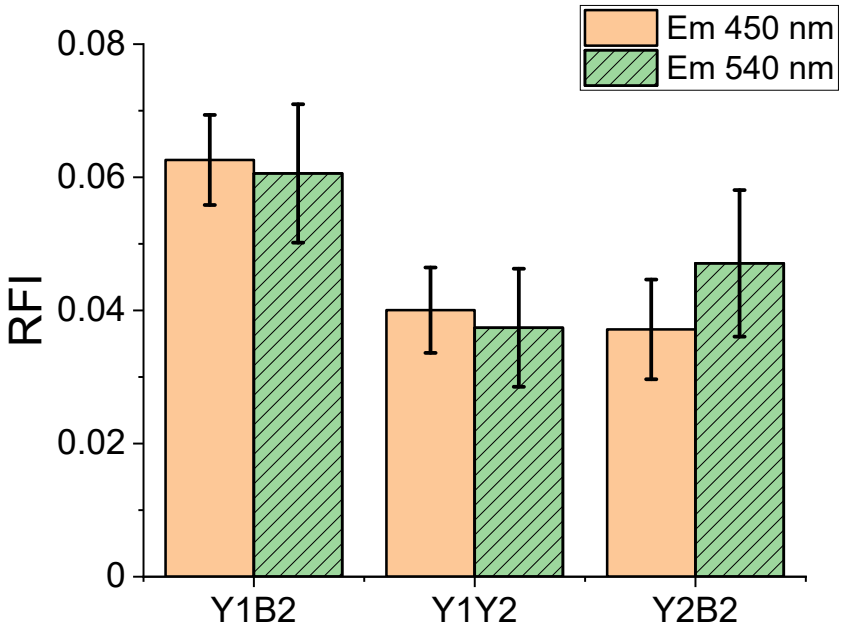

Supplementary Figure S8. Normalized, average change in intensity at 450 nm and 540 nm for a mixture of yCDs conjugated with ASO1 and bCDs conjugated with ASO2 (Y1B2), a mixture of yCDs conjugated with ASO1 and yCDs conjugated with ASO2 (Y1Y2), and a mixture of Y2 and bCDs conjugated with ASO2 (Y2B2) after excitation at 360 nm.

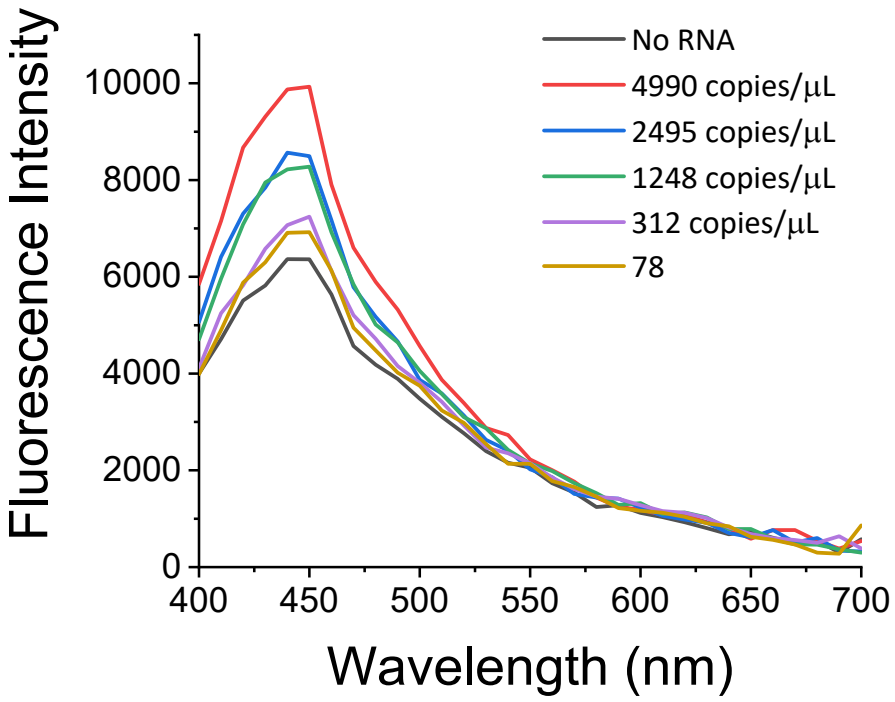

Supplementary Figure S9. Fluorescence intensity vs. wavelength plot showing the dependence of Y1B2's emission intensity on SARS-CoV-2 RNA concentration.

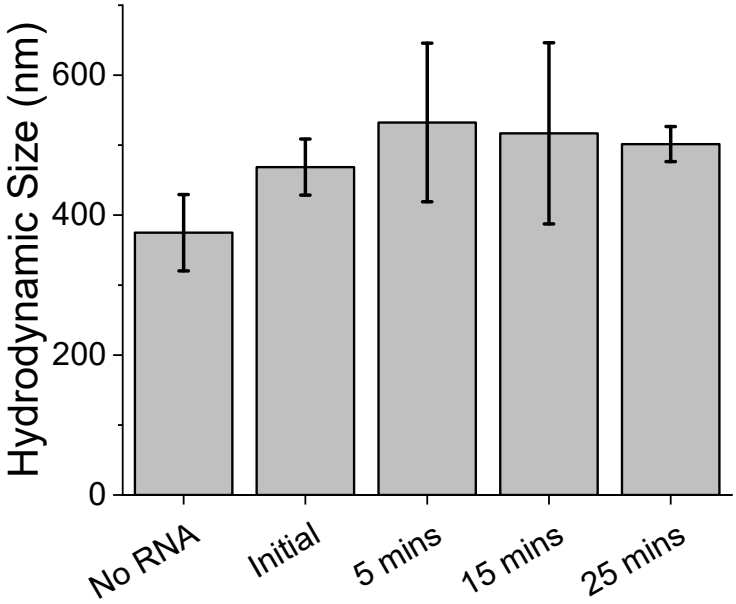

Supplementary Figure S10. The average intensity-weighted hydrodynamic sizes of Y1B2 particles at different time points after the addition of SARS-CoV-2 RNA.